REFERENCE 147

A. J. KIRSCHBAUM, "STUDIES OF ENRICHED URANIUM GRAPHITE REACTOR SYSTEMS," UNIVERSITY OF CALIFORNIA RADIATION LABORATORY REPORT UCRL-4983-T (NOVEMBER 1957).

UCRL-4983-T

UNIVERSITY OF
CALIFORNIA

Radiation Laboratory

LIVERMORE SITE

UCRL-4983-T

UNIVERSITY OF CALIFORNIA

Radiation Laboratory, Livermore Site

Livermore, California

Contract No. W-7405-eng-48

STUDIES OF ENRICHED URANIUM GRAPHITE REACTOR SYSTEMS

Albert J. Kirschbaum

November 1, 1957

Printed for the U.S. Atomic Energy Commission

STUDIES OF ENRICHED URANIUM GRAPHITE REACTOR SYSTEMS

Albert J. Kirschbaum

University of California Radiation Laboratory
Livermore Site

November 1, 1957

I. INTRODUCTION

This paper presents the results to date of a basic neutronic studies program at UCRL on enriched uranium graphite moderated reactor systems. The purpose of this program is twofold. First to supply valid critical data to be used in normalizing several multigroup codes that are being developed on the computing machines at Livermore. Second, to develop additional experimental techniques that will supply data for further checks on the accuracy of the calculational techniques. Pulsed source measurements appear to provide much additional data useful in code checking and in evaluating and understanding the neutronics of a reactor core.

This paper will present the critical mass and time behavior raw data. The results of checks for systematic errors, the reduction of some of the data to correspond to an idealized system, and comparison of the data with a naive but simple theory will be given. Most of the data is for bare systems, however, the raw data for several carbon and beryllium reflected systems is given also.

II. DESCRIPTION OF EXPERIMENTS FOR CRITICAL MASS STUDIES

See Figure 1 for a sketch of the low mass table and pictures of graphite blocks, foils, and a typical octagonal assembly. The low mass stacking table upon which the reactors were assembled consists of an 8' x 8' x 1' aluminum honeycomb slab rigidly supported by an aluminum stand. The honeycomb is made of 2 mil 2S aluminum foil in a 3/8" hexagonal cell lattice with a density of 3 lbs./ft^2. The table top is 4 feet from the floor. Over this table is suspended a 2S aluminum canister with 4 channels in X cross-section (each $\frac{1}{2}$" x 6" exterior dimension). Each channel guides a $\frac{1}{4}$" thick, 4' long boral element. Three of the elements (5" wide) are safety rods and the fourth (1" wide) is the control rod. A tube through the canister axis permits the insertion of various sources into the core. The safety rods are lifted by a conventional electromagnet arrangement; the control rod is screw driven.

Core material for the assemblies consists of thin graphite plates and nominally 1 and 2 mil thick enriched uranium foils. Using these plates and foils, a large number of geometries and carbon-uranium ratios can be built up.

The graphite plates were ATJ carbon machined in $\frac{1}{2}$" x 6" x 6" squares with a 10 mil recess milled on one side to accommodate the foils. Triangular blocks were formed by cutting square blocks diagonally. Blocks containing milled slots to provide 40% voids were also made. The blocks allow density

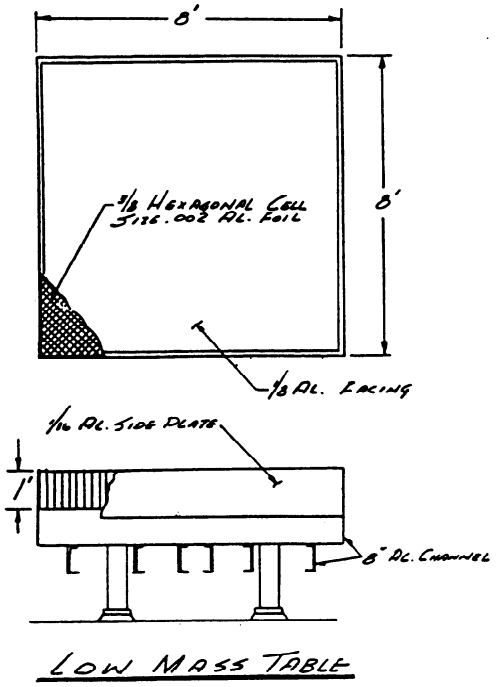

LOW MASS TABLE

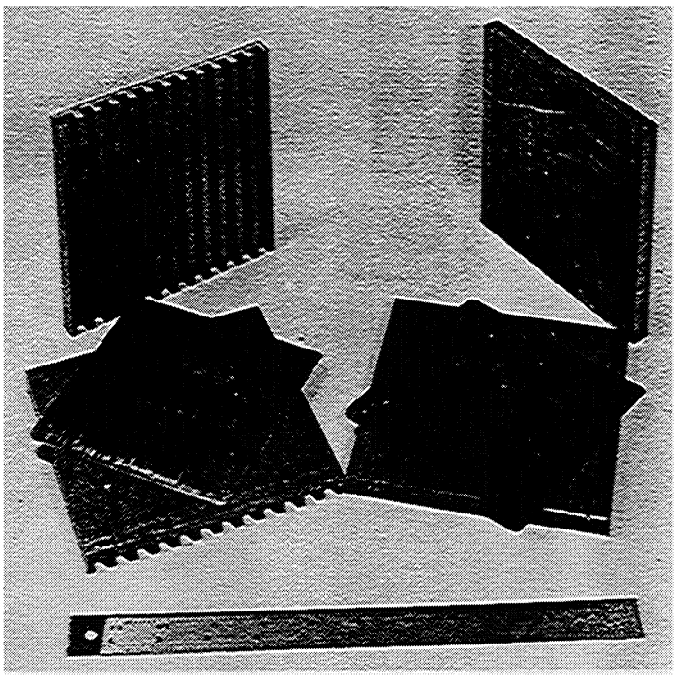

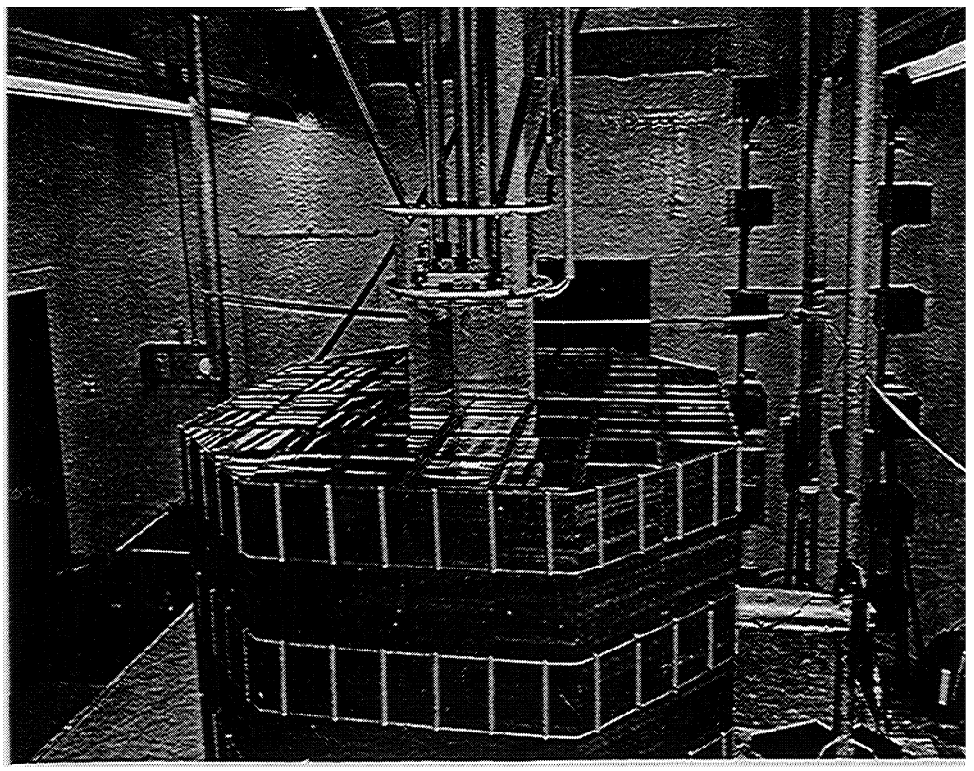

FIGURE I

changes in the core to be made by the proper ratio of full density and 60% density blocks. An analysis of the graphite is given below. A selection of 1 and 2 mil enriched uranium foils (93.5% U^{235}) in $5\frac{1}{4}$" squares and triangles were used for fuel. These foils are coated with a fluorocarbon plastic to prevent oxidation and contain fission products. Chemical analysis and danger coefficient measurements in the glory hole of the Water Boiler reactor indicate that this material has no appreciable absorption or moderating effect. The average plastic per square foil 0.920 grams.

ATJ Graphite Element	Density 1.73 gm/cc Parts per Million
B	14.4
Ca	200
Al	200
Mg	30
Fe	600
Ag	6
Cu	500
Ti	60

Instrumentation is standard throughout, using BF_3 ionization chambers connected either to Beckman micro-micro-ammeters or to log N amplifier period meters. Self-shielding due to the finite thickness of the foils was determined by irradiating sample foils of various thicknesses at various positions in the assembly and extrapolating specific activity back to zero foil thickness. Corrections for fission fragment loss from the foils was made. See Appendix I.

Cores with three carbon to uranium atomic ratios have been investigated so far. The actual ratios uncorrected for self-shielding are 600:1, 1200:1, and 2340:1. Self-shielding effects change these to 675:1, 1379:1, 2586:1, respectively. Throughout the report the numbers 600, 1200, and 2340 will be used where only identification of the loading concerned is required.

Five measurements of critical height for pseudo octagonal cylinders were made. The remainder are all rectangular parallelepipeds.

III. CRITICAL MASS DATA

Figure 2 shows appropriately labeled dimensions for the octagonal and rectangular core geometries. Corresponding core and reflector dimensions are given in Table I.

Table I lists all the critical mass data to date. Following Table I are notes giving further data on the lattices used and the remarks pertinent to some of the experiments.

Table II is a summary of the critical mass data with core conditions only approximately specified.

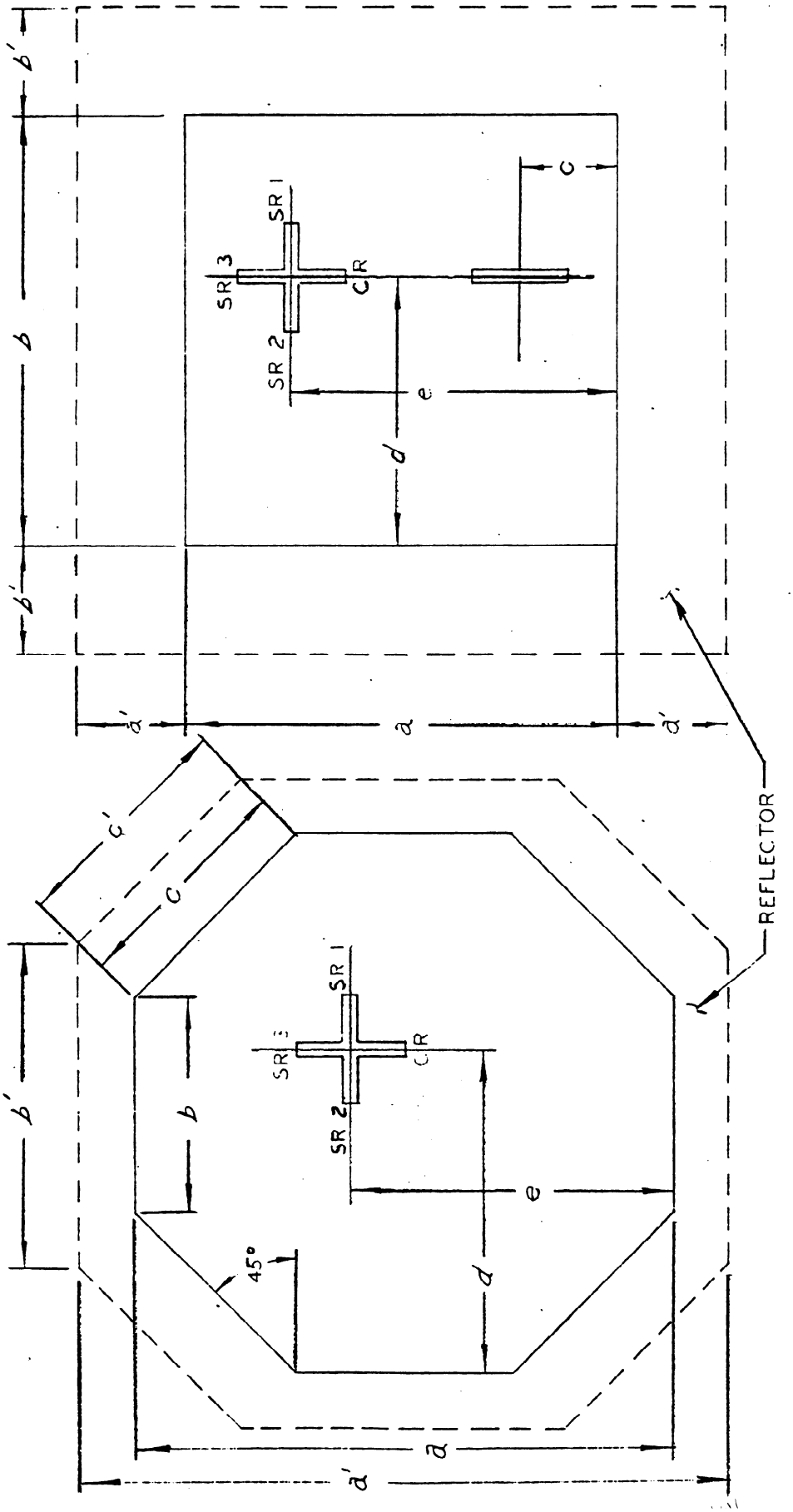
b'
b
b'
a'
a
a'
c
SR 1
SR 3
CR
SR 2
e
d
B
c'
c
REFLECTOR
b'
b
SR 1
SR 3
CR
SR 2
e
d
45°
a'
a
A

FIGURE 2

TABLE I

Assembly No.	Geometry	Reflector	Dimensions (inches) a	a'	b	b'	c	c'	d	e	Lattice	Critical Height (inches)	Critical Mass (kg) Core C	U^{235}	Core Al	Reflector	C/U^{235} Absolute	Effective	Remarks
1	A	*	60½	*	24½	*	25.5	*	30¼	30¼	a	33.8	2730	89.3	6.04	*	599	675	
2	"	"	54½	"	18½	*	"	"	24¼	24¼	"	38.8	2420	79.1	6.94	"	"	"	
3	"	"	48½	"	24½	"	17.0	"	"	"	"	42.3	2340	76.5	7.48	"	"	"	
4	"	"	42½	"	18½	"	"	"	18¼	18¼	"	(61)	(3430)	(112)	(10.9)	"	"	"	
5	"	C	36½	48½	12½	24½	"	17.0	"	"	"	44.3	1240	40.5	7.91	1210	"	+	I
6	B	*	48½	*	48½	*	*	*	24¼	24¼	b	40.0	2520	82.3	7.15	*	600	675	
7	"	"	"	"	"	"	"	"	"	"	c	42.4	2670	43.5	3.85	"	1200	1379	
8	"	"	"	"	"	"	"	"	"	"	d	42.3	"	43.6	3.86	"	"	"	II
9	"	"	"	"	"	"	"	"	"	"	e	42.5	2660	43.4	3.84	"	"	"	III
10	"	"	"	"	"	"	6.0	"	"	"	"	42.9	2690	44.1	3.90	"	"	"	IV
11	"	"	"	"	"	"	*	"	"	36¼	"	41.8	2640	43.1	3.81	"	"	"	V
12	"	"	"	"	"	"	"	"	"	42¼	"	41.4	2610	42.5	3.76	"	"	"	VI
13	"	"	"	"	"	"	24.0	"	"	"	"	42.3	2650	43.4	3.84	"	"	"	VII
14	"	"	"	"	"	"	"	"	"	"	"	42.3	2660	43.6	3.85	"	"	"	VIII
15	"	"	"	"	"	"	"	"	"	"	"	43.3	2730	44.5	3.90	"	"	"	IX
16	"	"	"	"	"	"	"	"	"	"	"	44.8	2830	46.1	4.08	"	"	"	X
17	"	C	"	0	36½	6.0	*	"	12¼	30¼	"	42.8	2030	33.0	3.88	667	"	+	XI
18	B	C	36½	6.0	36½	6.0	*	*	12¼	24¼	c	43.5	1550	25.3	3.95	1190	1200	+	XII
19	"	*	48½	*	48½	*	"	"	24¼	"	e	47.6	3000	25.1	4.33	*	2340	2586	
20	"	"	"	"	"	"	"	"	"	36¼	"	46.8	2960	24.7	4.26	"	"	"	V
21	"	"	"	"	"	"	"	"	"	42¼	"	46.4	2930	24.5	4.21	"	"	"	VI
22	"	"	"	"	"	"	6.0	"	"	"	"	46.9	2950	24.7	4.26	"	"	"	VII
23	"	Be	"	0	36½	3.0	*	"	18¼	30¼	"	48.1	2280	19.1	4.37	422	"	+	XI
24	"	"	"	"	"	6.0	"	"	"	"	"	40.9	1940	16.2	3.72	717	"	+	"
25	"	"	36½	6.0	"	"	"	"	"	24¼	"	36.8	1320	11.0	3.34	1130	"	+	XII

* Not applicable
\+ Undetermined
( ) Gross extrapolation

Notes Pertaining To Table I

LATTICE:

a. All core columns are constructed with one 2 mil Oy fuel foil recessed on top of each ½" thick ATJ graphite plate. The graphite plates are stacked with one 0.4 porosity plate (av. density = 1.03 gm/cm^3) beneath eleven non-porous plates (av. density = 1.70 gm/cm^3) beginning with a porous plate at the bottom.

Control system void/inch of core height	= 12¼ in^3/in
Control system aluminum/inch of core height	= 179 gm/in
Av. core porosity (excluding control void)	= 0.050
Overall graphite density (excluding cross void)	= 1.645 gm/cm^3
Overall U^{235} density	= 0.05345 gm/cm^3
Overall $(CF_2)_n$ density	= 0.0031 gm/cm^3

b. Same as "a" except for:

Overall U^{235} density	= 0.05334 gm/cm^3

c. Same as "a" except for:

One 2 mil Oy fuel foil recessed on top of very other ½" thick graphite plate beginning with the bottom plate.

Control system aluminum/inch of core height	= 91.0 gm/in
Overall U^{235} density	= 0.02667 gm/cm^3
Overall $(CF_2)_n$ density	= 0.0015 gm/cm^3

d. Same as "c" except that porous plates are randomized in position and orientation.

e. Same as "a" except for:

One 1 mil Oy fuel foil recessed on top of every other ½" thick graphite plate beginning with the bottom plate.

Control system aluminum/inch of core height	= 91.0 gm/in
Overall U^{235} density	= 0.01369 gm/cm^3
Overall $(CF_2)_n$ density	= 0.0011 gm

Notes Pertaining To Table I (Continued):

REMARKS:

I. No end reflectors.

II. Test for neutron streaming thru, and density inhomogeneity from, porous plate grooves. Effect negligible.

III. Test for thermal neutron reflection from vault. Entire core surrounded with $\frac{1}{4}$" thick boral sheet.

IV. Control system void axis aligned with core axis and a $\frac{1}{2}$" x 12" cross-sectional test void installed as indicated by dimension "c".

V. Control system void axis displaced 12" from core axis. No test void.

VI. Control system void axis displaced 18" from core axis. No test void.

VII. Control system void axis displaced 18" from core axis and a $\frac{1}{2}$" x 12" cross-sectional test void installed as indicated by dimension "c".

VIII. Test for core poisoning by control system aluminum. Remark VII with test void filled with aluminum (11.3 kg). Effect negligible.

IX. Investigate potentiality of Cd control in low epithermal systems. Remark VII with a 0.030" thick, 1" x 4' Cd strip inserted in test void.

X. Remark IX with a 0.030" thick, 3" x 4' Cd strip inserted in test void.

XI. Reflected on 2 sides. No end reflectors.

XII. Reflected on 4 sides. No end reflectors.

TABLE II

Core Size In Inches	Reflector Thickness In Inches	C/U Absol.	C/U Eff.	H_c Inches	U^{235} Kg	
60½" octog.	0	600	675	33.8	89.3	Pseudo Octagon
54½ "	0	600	675	38.8	79.1	
48½ "	0	600	675	42.3	76.5	
42½ "	0			~ 61	~112	
36½ "	~6-C-8 sides	600		44.3	40.5	
48½ x 48½	0	600	675	40.0	82.3	
48½ x 48½	0	1200	1379	42.4	43.5	
48½ x 36½	6-C-2 sides	1200		42.8	33.0	X off center
36½ x 36½	6-C-4 sides	1200		43.5	25.3	X off center
48½ x 48½	0	2340	2586	47.6	25.1	
48½ x 36½	6-Be-2 sides	2340		40.9	16.2	X off center
36½ x 36½	6-Be-4 sides	2340		36.8	11.0	X off center

IV. CORRECTION OF DATA FOR SYSTEMATIC ERRORS

The physical model we set out to investigate is a bare homogeneous graphite-oralloy system. Departures from this model are necessary in order to actually carry out the associated experimental program. The major departures are: the fuel is lumped into foils instead of being homogeneously distributed; gaps have to be provided for the safety and control rods required for safe operation; the actual system must be located in a vault or test cell and rest on a support table. To estimate the influence these experimental modifications have on system reactivity, a series of auxiliary experiments have been carried out. They can be summarized as follows:

C/U Absolute	Foil Thickness	Disadvantage Factor	C/U Effective
600	2.08	.889	675
1200	2.08	.870	1379
2340	1.06	.905	2586

The subject of the conversion of data on systems with lumped fuel foils to equivalent homogeneously loaded systems is covered in appendix on fuel foil self-shielding. The corrections deduced in appendix are incorporated in the final data of this report.

The graphite moderator is in the form of 6" x 6" x $\frac{1}{2}$" blocks. For convenience in stacking, two types of blocks are used; one at full graphite density, $\rho = 1.70$ gm/cm^2; the other with slots milled out, $\rho = 1.03$ gm/cm^2. In the lower density blocks, the milled slots allow the use of a lifting mechanism. Thus a stack is composed of a bottom low density block and 11 high density blocks above. The entire stack of 12 blocks is lifted at once with the lifting tool. The most straightforward method of building up the reactor is with entire horizontal planes of low density blocks appearing every 6 inches in height. To test whether these planes caused neutron streaming, one assembly was reloaded with the low density blocks randomized so that no horizontal low density plane existed. The critical height decreased by less than 0.1 inch, which must be considered within experimental precision. Compare assemblies 7 and 8 in Table I.

Neutron reflection from the test cell walls and floor was investigated by surrounding a critical system by low energy neutron absorbing boral sheet. The capture of these returning neutrons before they entered the reactor increased the critical height approximately 0.1 inch. Compare assemblies 7 and 9 in Table I.

Aluminum guides in control and safety rod voids have a negligible effect on system reactivity. This was established by inserting extra aluminum in the safety rod voids and observing no change in the system critical height. Compare assemblies 13 and 14 in Table I.

Critical Height Precision: The gross height increment is $\frac{1}{2}$ inch since this is the block thickness and changes are made by entire layers. However, extrapolations to critical with the data from four separate detection channels are consistent within .1 inches. Critical heights are quoted for all safety and control rods out of the core.

V. REDUCTION OF DATA TO AN IDEALIZED SYSTEM AND CORRESPONDING CRITICAL BUCKLINGS

A. Uncorrected Bucklings

ρ graphite = 1.645 excluding cross void

δ = 1.92 cm = extrapolation dist.

A formula for the relation between the buckling of a regular octagon and a circle of equal area has been derived.

$$B^2_{oct.} = 1.009\ B^2_{circle}$$

Using this and the usual formula for buckling of a cylinder, one obtains for the 600/1 octagons

Octagon	H_c	$B^2_{obs.}$
48.5"	42.3"	20.96×10^{-4}
54.5"	38.8"	20.99×10^{-4}
60.5"	33.8"	21.26×10^{-4}

For the bare rectangular parallelepipeds all $48\frac{1}{2}$ square one obtains

C/U eff.	H_c	B^2_{axial}	$B^2_{obs.}$
675	40.0	8.88×10^{-4}	21.11×10^{-4}
1379	42.4	7.98×10^{-4}	20.17×10^{-4}
2586	47.6	6.34×10^{-4}	18.57×10^{-4}

B. Corrected Bucklings

The above bucklings ignore the effect of the control system cross void. The effect of this void was determined three ways.

1. The changes in critical height as the center of the cross was moved 12" and 18" off center were measured. See assemblies 7, 11, 12 and 19, 20, 21 in Table I. Extrapolating to the center of the cross just on the edge of the core gives a percentage change in height of:

3.1% for 1200/1 $\quad \Delta H_c = 1.3"$

3.3% for 2340/1 $\quad \Delta H_c = 1.6"$

Assuming an average decrease of 3.2% in critical height as the effect of removing the cross void, new bucklings can be calculated. They are given in Table III.

An experiment was done on the 1200/1 system in which the full cross void was placed 18" from the center and an additional ½ cross void was placed at the center (assemblies No. 12 and 13). The increase in H_c associated with the half cross void was 0.9". If one assumes that the full cross effect is just double the half cross effect, one arrives at a $\Delta H_c = 1.8"$ for the full cross in the center. This $\Delta H_c = 1.8"$ is to be compared with the $\Delta H_c = 1.3"$ above arrived at by extrapolation. The agreement is poor.

2. Consider the cross void as a unit perturbation, δ, on the critical buckling, which we weigh at various positions by the flux squared.

$$B^2_{observed} = B^2_o - \varphi^2 \delta$$

B^2_o is the buckling without the cross void perturbation. Substituting the observed bucklings for the three cross void positions in this equation, and solving for the best values of δ and B^2_o, one obtains

$$1200/1 \qquad \delta = .48 \times 10^{-4} \qquad B^2_o = 20.62 \times 10^{-4}$$

$$2340/1 \qquad \delta = .41 \times 10^{-4} \qquad B^2_o = 18.97 \times 10^{-4}$$

Both values of B^2 represent a 2% increase in the critical buckling for removal of the cross void. These values are included in Table III.

3. 2-group Perturbation Treatment: A slightly more sophisticated treatment involves the use of 2-group perturbation theory. The steps followed are:

a. Adjust 2-group constants to give k = 1 for observed B^2.

b. Calculate $\delta k/k$ for perturbation caused by cross void in center. The effect of the void is considered as a reduction in density of the central 12" x 12" section of core graphite.

c. Relate $\delta k/k$ to the change in buckling using Age theory.

The results of this calculation are also given in Table III.

TABLE III

$(C/U)_{eff}$	Observed H_c"	Observed B^2	Correction by extrapolation of cross motion H_c	Correction by extrapolation of cross motion B^2	Correction by φ^2 perturbation H_c	Correction by φ^2 perturbation B^2	Correction by 2-group perturbation H_c	Correction by 2-group perturbation B^2
675	40.0	21.11×10^{-4}	38.7	21.69	39.0	21.53	38.8	(21.64)
1379	42.4	20.17	41.0	20.69	41.2	20.62	41.0	20.68
2586	47.6	18.57	46.1	18.98	46.1	18.97	45.9	(19.04)

C. Comparison With Modified Fermi Age Theory

The probability of a neutron escaping capture by U^{235} in slowing down is relatively small for the fuel rich system C/U = 675, but gets progressively better as the fuel becomes more dilute. The Fermi Age equation for a graphite moderated system in which the neutrons are captured at thermal energies is:

$$k = \frac{k_\infty e^{-\tau B^2}}{1 + L^2 B^2} \qquad \text{where } \tau \text{ is computed down to thermal energy } \tau(E_o, E_{th}) \qquad (1)$$

Another formulation utilizing the Fermi slowing down model is to assume that no neutrons reach thermal energy but all neutrons are captured at some single higher energy E_i. Then

$$k = k_\infty e^{-\tau(E_o, E_i)B^2} \qquad (2)$$

TABLE IV

$(C/U)_{eff}$	B^2 at ρ=1.645	E_i	$\tau(E_o,E_i)$	k_∞	$k=k_\infty e^{-\tau(E_o,E_i)B^2}$	$\frac{k=k_\infty e^{-\tau(E_o,E_{th})B^2}}{1 + L^2 B^2}$
675	21.64×10^{-4}	.15 ev	313.6	1.98	1.006	.931
1379	20.68	.11	318.1	1.99	1.033	.948
2586	19.04	.09	321.1	1.97	1.071	.962

This average capture energy E_i can be chosen to correspond with the average capture cross section in our self-shielding oralloy foils. Table IV shows that for the fuel rich system C/U = 675, the modified Fermi age equation (2) works very well but gets progressively worse as the fuel becomes more dilute. This is reasonable because our assumption of no thermal neutrons becomes increasingly bad. On the other hand, worse results are obtained if we use the thermal energy model (1).

Another simple model can be constructed by combining the two simple models above. The probability of a neutron reaching thermal energy can be considered as the probability of being captured in U^{235} during slowing down. We can then assume that all neutrons captured during slowing down are captured at our previous energy E_i. We then have two types of neutron captures and combine the k's, weighting by the respective number of neutrons.

p = prob of reaching thermal energy in ∞ medium

$$k = (1-p)k_\infty(E_i)\, e^{-\tau(E_i)B^2} + p\, k_\infty(E_{th})\, \frac{e^{-\tau(E_{th})B^2}}{1 + L^2 B^2}$$

C/U	p using $\int \sigma_{235} \frac{dE}{E}$ = 1345b	k
675	.0723	1.000
1379	.2764	1.009
2586	.5037	1.016

VI. DESCRIPTION OF PULSED SOURCE MEASUREMENTS

The pulsed source consists of a deuterium ion source of the Phillips-Ion-Gauge type, extraction and focus electrodes, and a target electrode whose potential is variable up to 100 kv. The target is a tritium-loaded tungsten disk, the D-T reaction producing 14 Mev neutrons. Both pulse width and repetition rate are variable up to a duty cycle of 1%. The maximum integrated yield is 10^7 neutrons/sec.

The detector used is an enriched Li^6I crystal ($1\frac{1}{2}$ in. diameter, 1/8 inch thick) and 6655 photomultiplier; this system was chosen for its high efficiency and small size.

A block diagram of the time analyzer is shown in Figure 3. Data collection begins when the sawtooth ramp is triggered by the timing pulse from the pulsed source. The timing pulse may be delayed to permit counting during any portion of the source cycle. Counting time, or ramp length, is variable from 30 μsec. to one second. Detector pulses, after passing a single-channel differential pulse height analyzer which essentially passes only neutron pulses, are fed into the mixer circuit with the ramp. The mixer output is a pulse whose height is proportional to ramp height at the time of arrival of a neutron pulse. The time spectrum of neutron pulses is thereby changed to a height spectrum; data is presented on a 20-channel pulse height analyzer.

Calibration is made directly in time, by simulating detector pulses with a sliding calibrator pulse whose delay following ramp initiation is accurately known. A tektronix type 534 oscilloscope served this purpose; a variable delay pulse output is available, the calibration of which may be checked with a crystal-governed timing pulse generator. Pulse height analyzer gain and discriminator controls are used to adjust channel widths to the desired values, as indicated by the calibrator pulse.

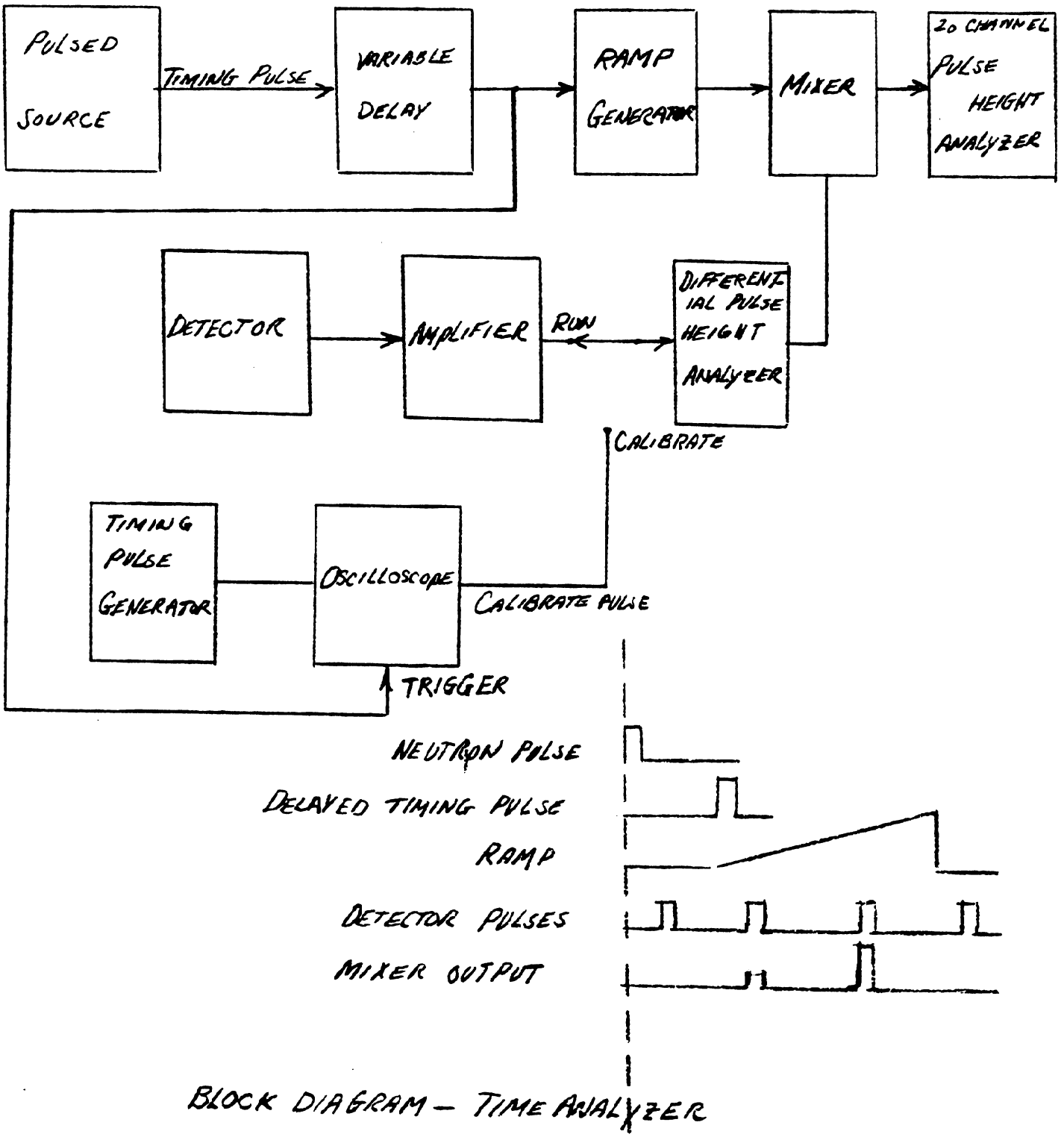

BLOCK DIAGRAM – TIME ANALYZER

FIGURE 3

Channel widths may be set up to within $\pm \frac{1}{2}\%$ by this method. It was found that during an average counting run (15 minutes), the average channel drift was about 1%.

The dead time of the system is about 20 μsec following each pulse. The dead time corrections, at the count rates used, were small compared to statistical inaccuracies, drifts, etc., and were therefore not applied

For background measurements a pair of gated scalers were used which counted neutron pulses at a variable position late in the cycle. The time widths of these channels were several times that of the prompt decay analyzer channel widths, so that satisfactory counting statistics were obtained. The wider channels are permissible since the count rate late in the cycle is essentially constant.

During data collection the source target was positioned at half reactor height; the detector at one-third reactor height, on an adjacent face. These positions were chosen in order to minimize contributions to the observed decay from higher-order modes in the neutron distributions. (Actually no evidence of non-fundamental modes was found; i.e., the measured decay constant of a system was independent of detector position over the central portion of the reactor.)

Figure 4 shows a typical set of counting data from a C/U-600 system. It is seen that after background subtraction the prompt decay exhibits curvature indicating an apparent insufficient background correction. This is believed due to the fact that the pulsed source target is outside the system. It is possible for neutrons leaving the target to be reflected into the system at a later time by the concrete walls of the room. The room thereby constitutes an extended though weak source of neutrons; a decay constant measurement with the assembly removed indicated exponential decay with a period of about two milliseconds for the room reflected neutrons. (The system center is six feet above the concrete floor, ten feet from concrete room walls on three sides and twenty feet on the fourth side). In subsequent tests on C/U-1200 systems it was possible to enclose the system completely in a boral shield, boral being a sandwich of aluminum and normal boron. The room reflected neutrons were thereby minimized and curvature of the prompt decay data was diminished. See Figure 5.

VII. DISCUSSION OF PULSED SOURCE DATA

Figures 6, 7, and 8 give plots of the prompt decay constants versus the buckling for the three systems 600/1, 1200/1, 2340/1. Table V gives the same data in tabular form.

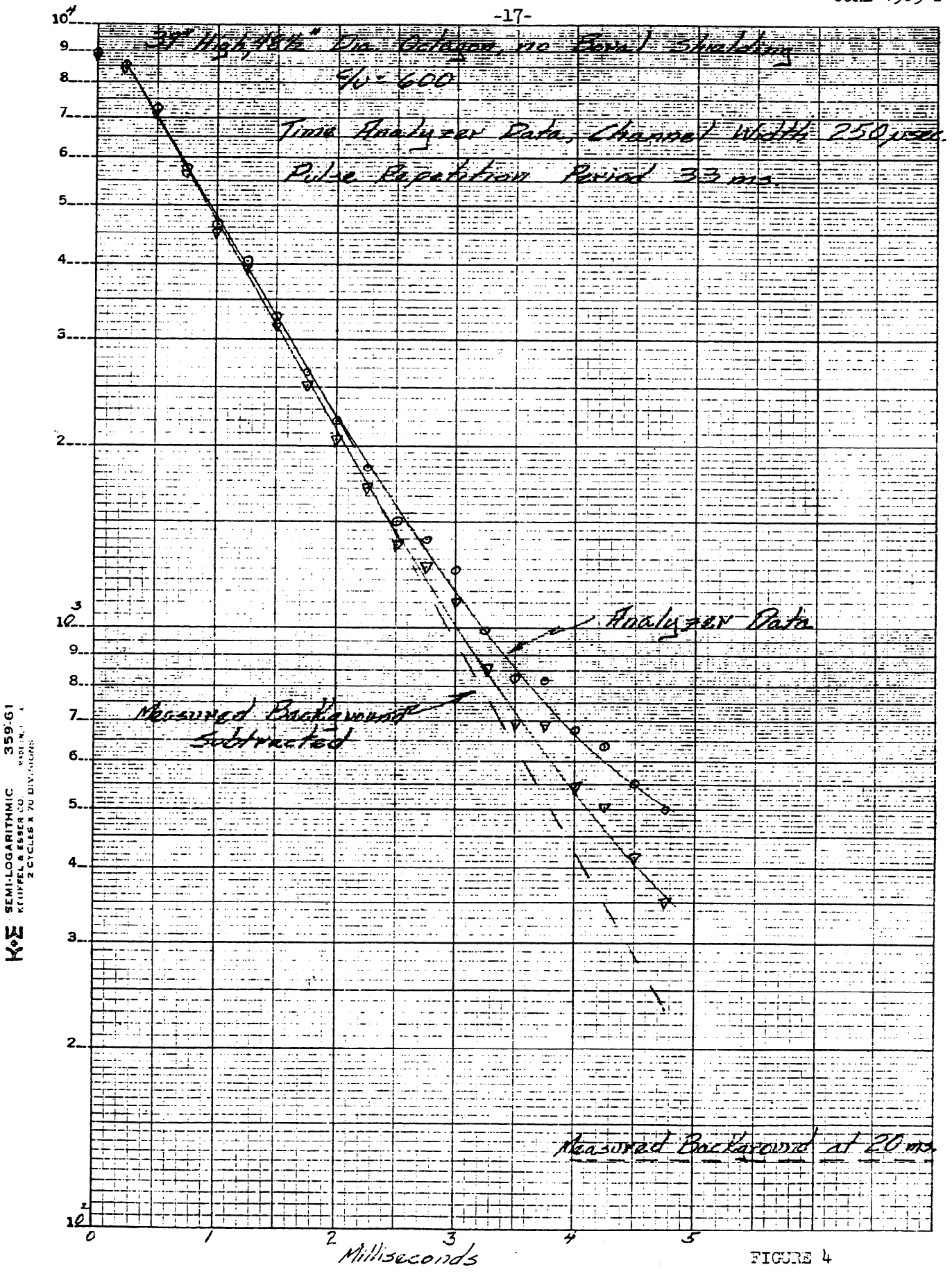
37" High, 18½" Dia. Celotex no Form / Shielding
Ge - 600
Time Analyzer Data, Channel Width 250 μsec.
Pulse Repetition Period 33 ms.
Analyzer Data
Measured Background Subtracted
Measured Background at 20 ms
Milliseconds
SEMI-LOGARITHMIC 359-61
KEUFFEL & ESSER CO.
2 CYCLES X 70 DIVISIONS

FIGURE 4

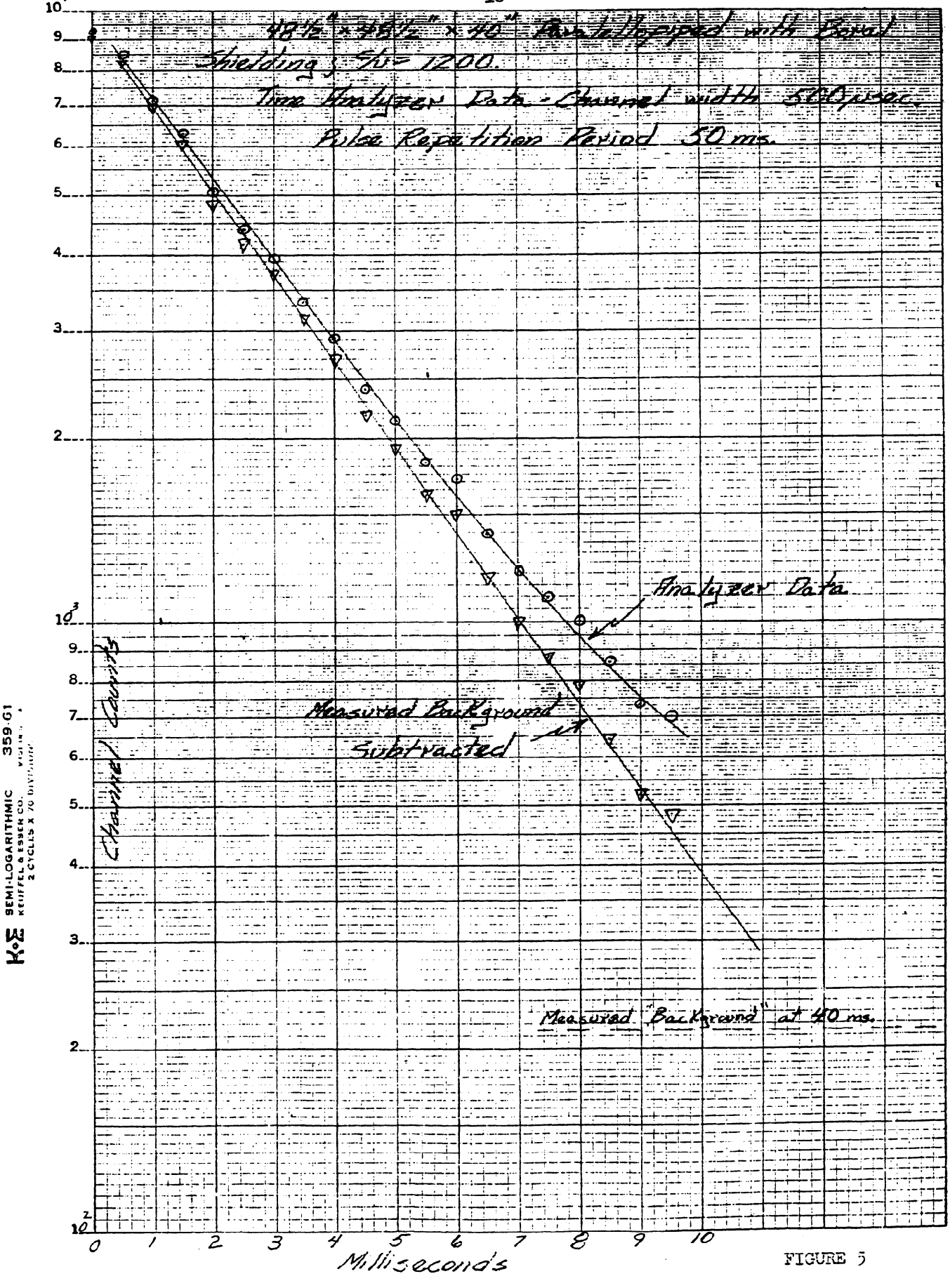
40½" x 48½" x 40" Fe stepped with Lead Shielding; Su = 1200.
Time Analyzer Data - Channel width 500 μsec.
Pulse Repetition Period 50 ms.
Analyzer Data
Measured Background Subtracted
Measured Background at 40 ms.
Channel Counts
Milliseconds
0 1 2 3 4 5 6 7 8 9 10
10⁴ 9 8 7 6 5 4 3 2
10³ 9 8 7 6 5 4 3 2
10²
K&E 359-61 SEMI-LOGARITHMIC KEUFFEL & ESSER CO. 2 CYCLES X 70 DIVISIONS

FIGURE 5

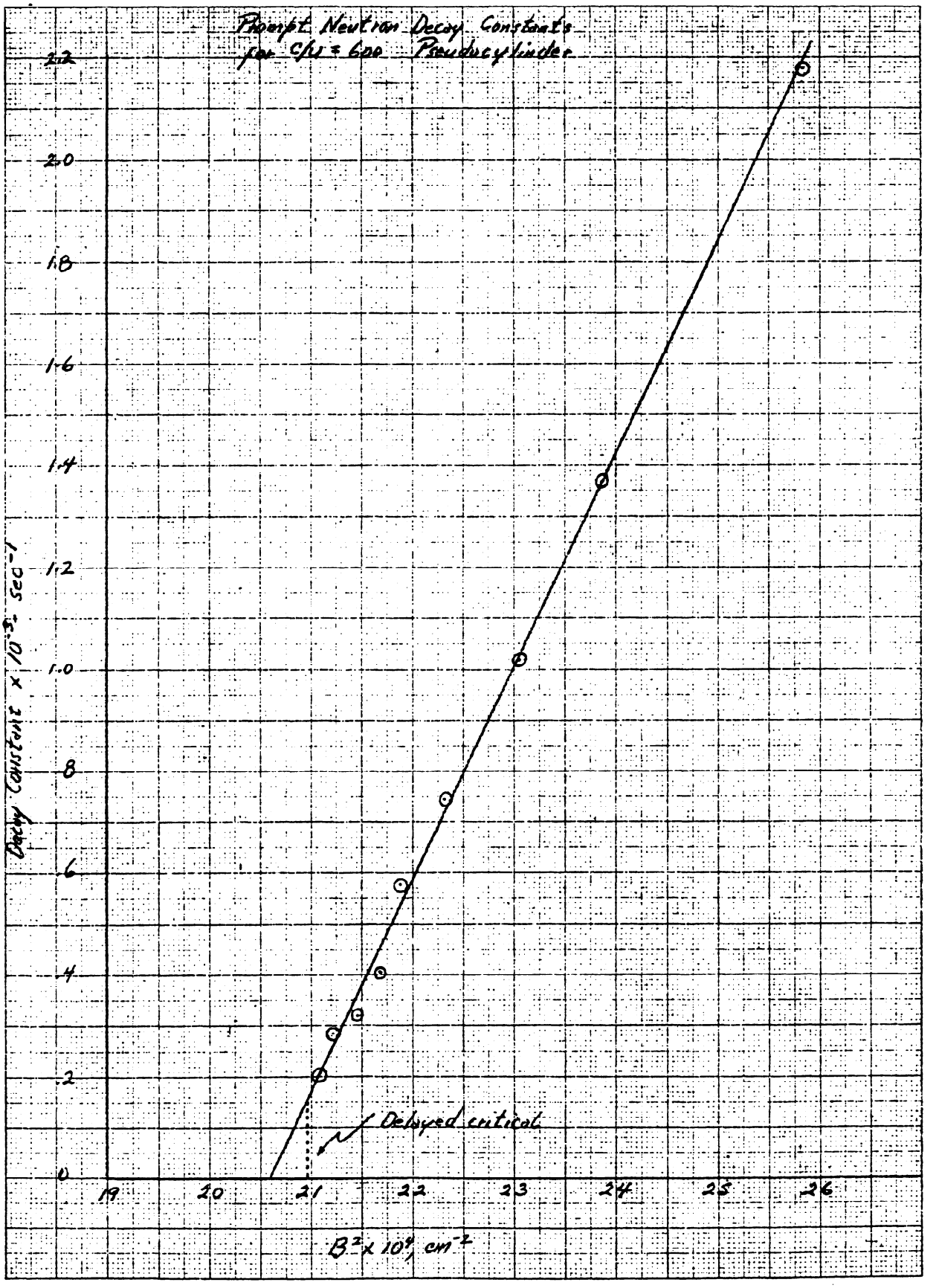

Fig 6

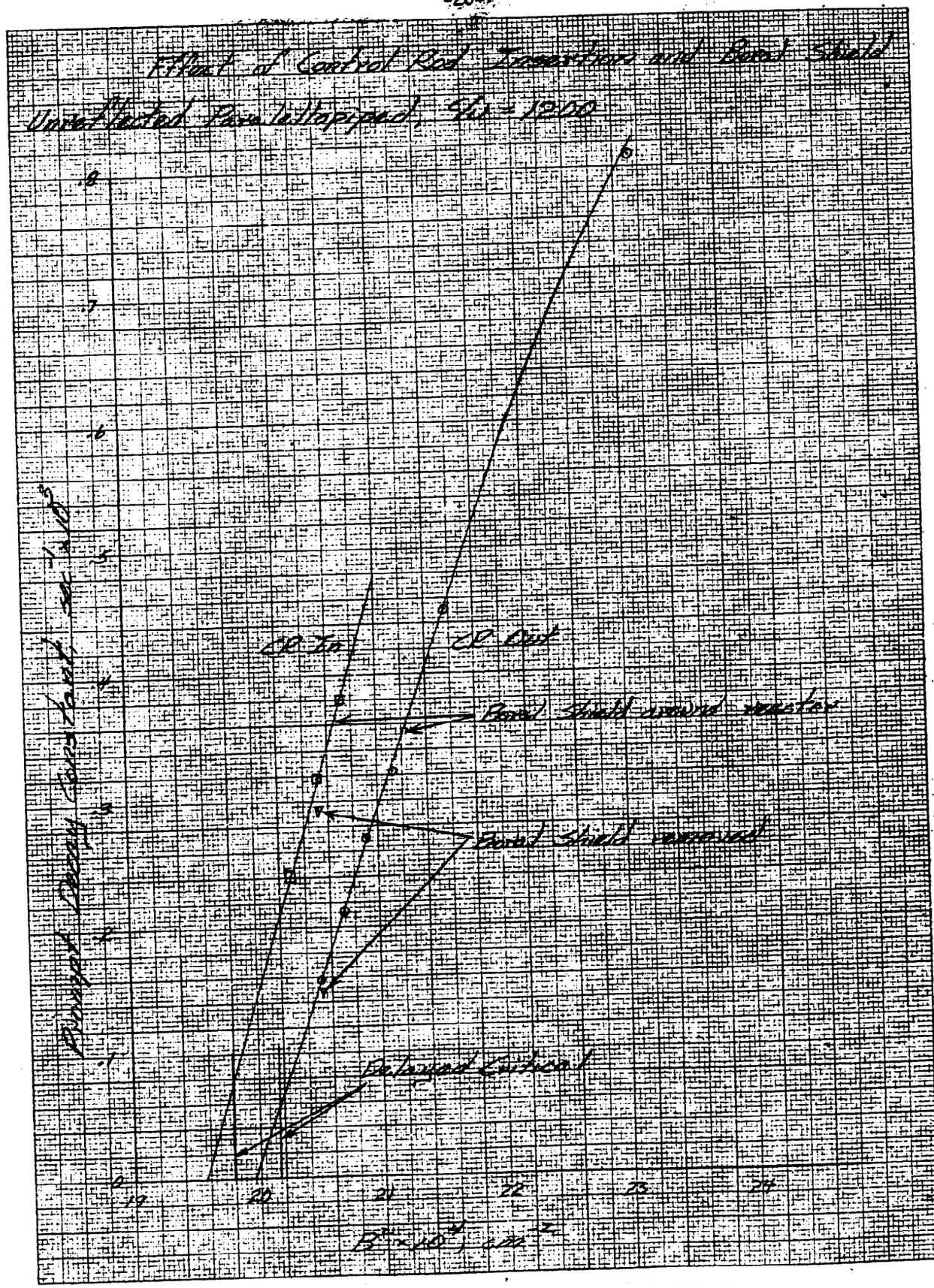

FIGURE 7

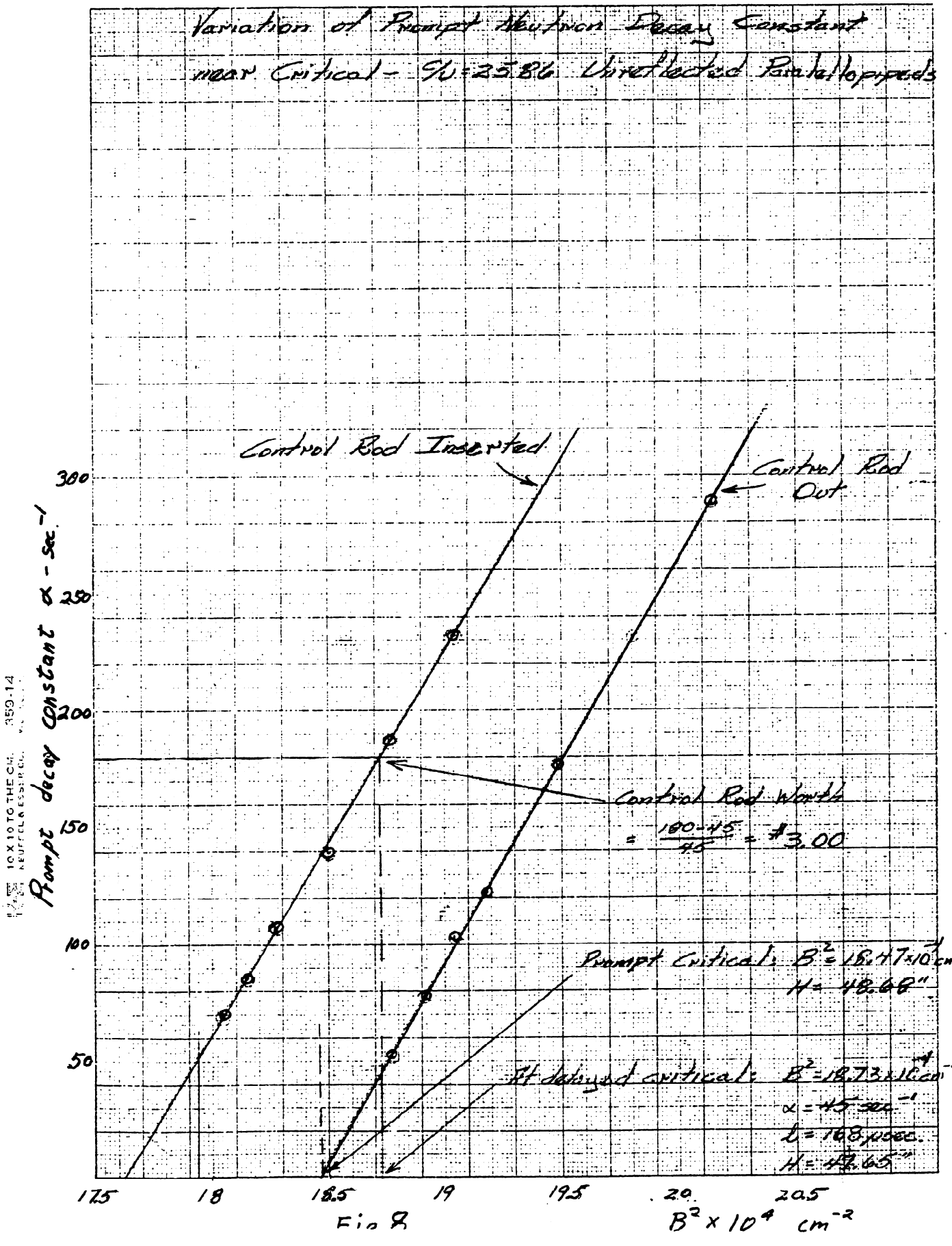
Variation of Prompt Neutron Decay Constant
near Critical - SV-2586 Unreflected Parallelopipeds
Control Rod Inserted
Control Rod Out
Control Rod Worth
= 160-45/45 = 3.00
Prompt Critical: B² = 18.47×10⁴ cm⁻²
H = 48.68"
If delayed critical: B² = 18.73×10⁴ cm⁻²
α = 45 sec⁻¹
ℓ = 168 μsec.
H = 49.65"
Prompt decay constant α - sec⁻¹
300
250
200
150
100
50
17.5
18
18.5
19
19.5
20.
20.5
B² x 10⁴ cm⁻²
10 X 10 TO THE CM. 359-14
KEUFFEL & ESSER CO.

Fig. 8

TABLE V

MEASURED DECAY CONSTANTS

Pseudocylinders, $C/U^{235} = 600$

Core Height Inches	$B^2 \times 10^4$ (cm^{-2})	Decay constants sec^{-1}
30	28.52	3130
33	25.96	2180
36	23.99	1370
37.5	23.17	1020
39	22.44	745
40	22.00	578
40.5	21.80	406
41	21.58	320
41.5	21.36	285
42	21.20	202

Unreflected Parallelepiped, $C/U = 1200$

Core Height Inches	$B^2 \times 10^4$ (cm^{-2})	Decay constants sec^{-1}
32	25.86	1470
36	23.11	811
39	21.56	448
40	21.12	316
40.5	20.90	274
41	20.71	207
41.5	20.51	154
42		

α's For 2340

	Core Ht.	$B^2 \times 10^4$	α, sec^{-1}
(delayed crit.)	47.65	18.56	
	47.5	18.60	52
	47	18.73	77
	46.5	18.67	102
	46	19.01	121
	45	19.30	176
	44	19.62	231
	43	19.95	288

If a least squares fit of the data is made to an equation of the form $\alpha = a + b B^2$, the resulting equations for the three cases are

600/1 $\alpha = -8571 + 4.163 \times 10^6 B^2$

1200/1 $\alpha = -5567 + 2.789 \times 10^6 B^2$

2340/1 $\alpha = -3183 + 1.739 \times 10^6 B^2$

The corresponding prompt critical bucklings are:

	Prompt Critical	Delayed Critical
600/1	20.59×10^{-4}	21.11×10^{-4}
1200/1	19.96×10^{-4}	20.17×10^{-4}
2340/1	18.30×10^{-4}	18.57×10^{-4}

Note that the delayed to prompt critical δB^2 are not very consistent. This is believed due to errors in the data. An effort is being made to improve the techniques to reduce this inconsistency in the results of this sensitive test of the data.

Results of decay constant measurements on carbon systems (ρ=1.64 gm/cm^3) are shown in Figure 9. Test systems were parallelepipeds in all cases.

A least square fit to the data yields:

$$\alpha = 181.5 + 1.94 \times 10^5 B^2 \text{ sec}^{-1}$$

In terms of moderator diffusion constants, the expression for α takes the form

$$\alpha = \Sigma_a v + Dv B^2$$

where $\Sigma_a v$ is the macroscopic absorption rate per unit volume, D the diffusion constant, and B^2 the geometrical buckling. An extrapolation distance of 1.92 cm was used in calculations of B^2.

The value of $\Sigma v = 181.5$ sec^{-1} is extremely high for graphite and is attributed to a boron impurity. Assuming the absorption cross-section for carbon to be 3.2 mb. at 2200 m/sec, it is found that the atomic boron/carbon ratio must be 13×10^{-6} to account for the measured absorption rate. Spectroscoptic determinations of the impurities present yielded boron/carbon atomic ratios from three random samples as the value resulting from the pulse experiment is in good agreement with these values.

The indicated diffusion constant, $Dv = 1.94 \times 10^5$ cm^2 sec^{-1}, is in reasonable agreement with the value of Antanov, et al*,(1.98×10^5 cm^2 sec^{-1}.) The diffusion length is given by $B_0^2 = \frac{1}{L^2}$, where B_0^2 is that for $\alpha = 0$.

---

* Antanov et. al., Peaceful Uses of Atomic Energy, Paper 661, Vol. 5

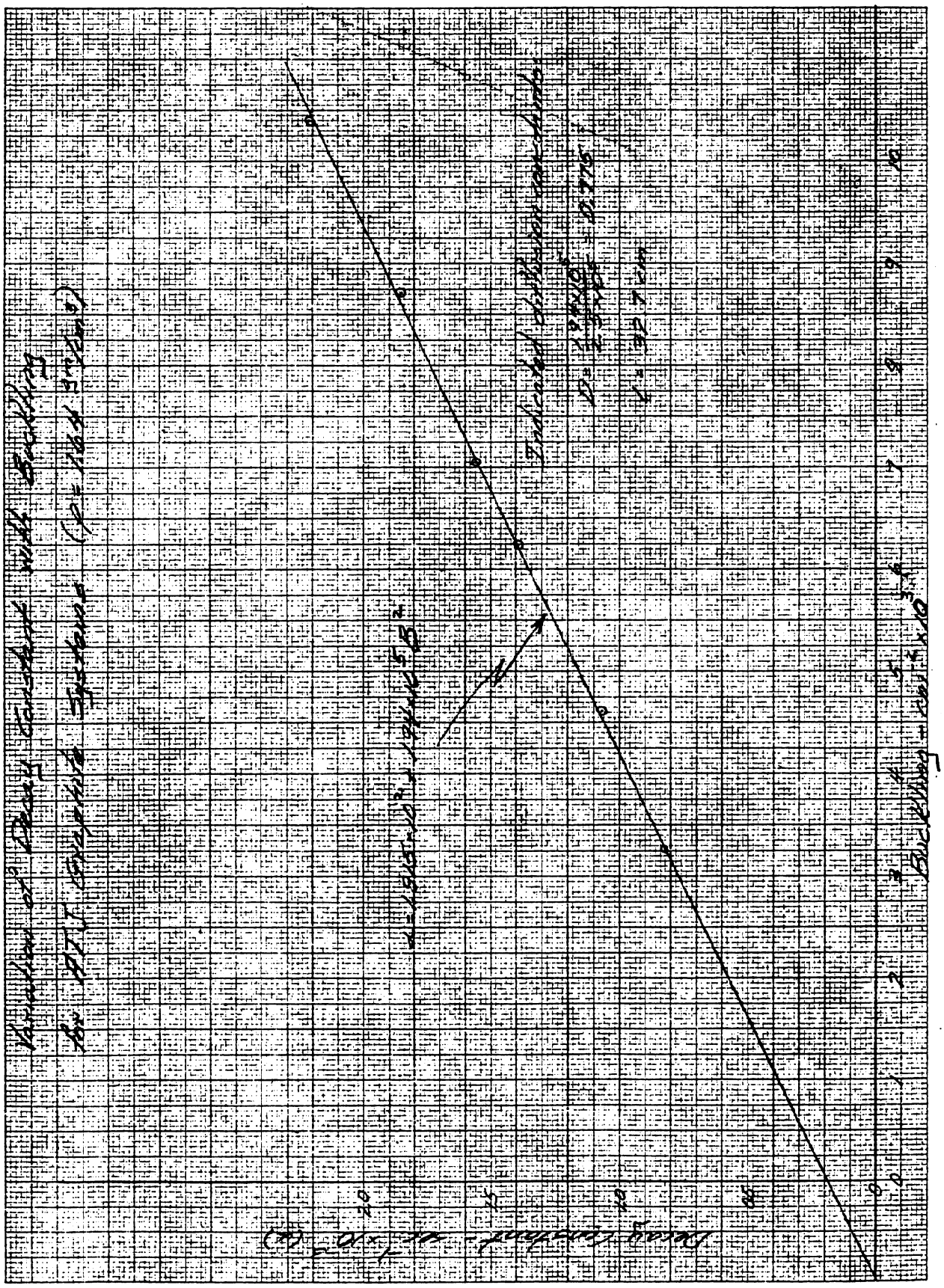

FIGURE 9

The result is L = 32.7 cm, considerably less than the accepted value of 50.2 cm; this is presumably due to the high boron content of the ATJ graphite.

Comparison of the pulsed measurements data with a simple theoretical model can be made. We derive an expression for α in the following manner:

1. Assume the neutron spectrum does not change during the decay after transients die out.

2. Consider the neutrons between energies E and E + dE, written as N(E) dE.

3. Let s be the average time required for a neutron to slow down from fission energy and be captured, i.e., the average time between fissions.

4. Now we write the relation between the prompt neutrons in dE at time t and at time t + s.

$$N(E,t+s) = N(E,t)\, e^{-\tau(E,E_c)B^2}\, k_\infty (1-\beta) e^{-\tau(E_f,E)B^2} = N(E,t) k_\infty (1-\beta)\, e^{-\tau(E_f,E_c)}$$

where

E_f = energy of fission neutrons

E_c = average energy at which neutron is absorbed.

We know experimentally:

$$N(t+s) = N(t)\, e^{-\alpha s}$$

$$\therefore\ e^{-\alpha s} = k_\infty (1-\beta)\, e^{-\tau B^2}$$

or

$$\alpha = -\frac{\ell n\, k_\infty (1-\beta)}{s} + \frac{\tau B^2}{s}$$

We compare this with the least square fits to the decay constant data. Using the first term allows us to evaluate s, and the second term gives τ.

$k_\infty = 1.98$ $\beta = .0075$

C/U	s in μsec	τ in cm^2
600/1	80	330
1200/1	122	340
2340/1	214	370

The simple model begins to break down for the highest C/U ratio system since it is approaching a thermal reactor. s has a diffusion time added to the slowing down time, and τ becomes the migration area.

Since $k = k^{\infty} e^{-B^2\tau}$

$$B^2\tau = \ln k^{\infty} - \ln k$$

$$\therefore \alpha = \frac{-\ln (1-\beta) - \ln k}{s}$$

which can be reduced to

$$\alpha = \frac{\beta-\rho}{s} \quad \text{for } k \approx 1$$

$$\text{and } \rho = \frac{k-1}{k}$$

This relation can be used to measure the reactivity effects of control and safety rods in large steps, i.e., up to 10% in k.

A P P E N D I X

SELF-SHIELDING

W. S. Gilbert

The reactor systems whose critical parameters we wish to determine are homogeneous mixtures of fuel and moderator, in our case oralloy and graphite. The physical approximation we have made to this model consists of alternate layers of fuel foils and moderator plates. This fuel lumping results in two interrelated effects; a fine structure modification to the spatial flux distribution with a periodicity determined by the fuel foil spacing in the lattice, and a self-shielding effect within the fuel foil itself. The fine structure imposed on the flux distribution is measurably small and its effect on system reactivity is to first order negligible. The fuel atom self-shielding within the fuel foil is, on the other hand, a relatively large effect and must be corrected for.

On the basis of first collision theory, one can arrive at a simple determination of the self-shielding factor for monoenergetic neutrons incident upon regular geometrical shapes with an isotropic angular distribution(1). For a purely absorbing infinite slab of thickness U in mean free paths, the disadvantage factor is: (2)

$$D.F. = \frac{1}{2u}\left[1 + (u-1)\, e^{-u} - u^2 \int_u^\infty e^{-y}\, \frac{dy}{y}\right]$$

The disadvantage factor times the actual atomic absorption cross section is equal to the average effective absorption cross section for the fuel. Or, the equivalent amount of fuel in our desired homogeneous system is equal to the disadvantage factor times the actual amount of fuel in our lumped fuel system.

$$\therefore \quad (C/U)_{\text{effective}} = \frac{(C/U)_{\text{nominal}}}{D.F.\ (\text{fuel foil})}$$

To experimentally determine the D.F. for our fuel foils, we irradiate small oralloy foils of different thicknesses in a uniform neutron flux region in the critical assembly of interest. The capture of neutrons in the fuel results in fissions whose fission fragments are mainly retained in the foils.

---

(1) Self-absorption of Monoenergetic Neutrons, W. J. C. Bartels, KAPL-336

(2) AM-509, Table of the Integral That Appears in The Evaluation of The Disadvantage Factor.

MT-1, G. Placzek, The functions $E_n(x) = \int_1^\infty e^{-xu}\, u^{-n}\, du$

Some of these fission fragments are γ-emitters and we use the γ-emission intensity as a measure of foil activation or absorption. The γ's are counted in a NaI scintillation spectrometer and the β's are shielded out. The foil specific activity per unit thickness is plotted vs. the foil thickness, and this curve is extrapolated and normalized to 1 at zero thickness. This is the foil disadvantage factor vs. foil thickness curve. By choosing a thickness corresponding to our fuel foils, we can determine the appropriate disadvantage factor to use. Before displaying these experimentally determined curves for systems of different fuel concentrations, a major correction to the raw counting data will be discussed.

Our monitor foils are clean oralloy disks with no surface covering. Fission fragments have varying ranges in uranium and a fraction of them escape through the foil surface. The fraction of the fragments escaping to the total produced in the foil depends upon the foil thickness. Data by Segre and Wiegand[3] has been approximately confirmed through the use of aluminum catcher foils. We correct our observed activation by a factor derived from their data.

$$(\text{Act})_{\text{corrected}} = \frac{T + .10}{T} \quad (\text{Act})_{\text{observed}}$$

where T is the foil thickness in mils.

The relative specific foil activations can be determined to a precision of $\pm$ 1½% although some of the data for earlier systems are considerably worse. The details of the counting system and data reduction will appear elsewhere.

For a source of thermal neutrons, we used a reactor consisting of a small graphite-oralloy core heavily reflected by D_2O. The self-shielding or monitor foils were placed in the D_2O 16" from the core edge. Though highly moderated and yielding a cadmium ratio of approximately 100, these neutrons were not all truly thermal. The average excess energy is small and unknown, pending further experiments. We refer to this data as our "thermal" disadvantage factor curve (Figure 10). The flux depression in the D_2O is somewhat different from that in the graphite, and so the D.F. curve for thermal neutrons in graphite might differ from that shown in Figure 10. Fortunately, the self-shielding effect is large compared with the flux depression effect and so one can sidestep a most knotty problem, i.e., does the experimentally determined D.F. curve correct only for self-shielding or does it include both the self-shielding and the flux depression effect. It is my opinion that our D.F. curves include both self-shielding and flux depression corrections although in some cases only a partial correction is made for the flux depression. Since our systems are comparatively fuel rich, our thermal utilization is very nearly unity despite small flux depressions. This is one of the reasons why the above question can be answered either way without making a significant difference in the deduced equivalent fuel loading

Our fuel foils are 5¼" x 5¼" as compared with our graphite moderator blocks which are 6" x 6". Thus our fuel forms a three dimensional lattice in

---

(3) Segre and Wiegand, Phys. Rev. 70, pg 808

the graphite moderator rather than the simpler one dimensional systems of fuel sheets separated by graphite indicated earlier. In the plane of the fuel foils, the flux depression is greater than transverse to the plane. Relative flux values are shown in the fuel foil plane in Figure 11. The activations have been divided by the expected $\cos\left(\frac{\pi}{2}\frac{x}{x_o}\right)$ distribution. The maxima correspond to the points midway between the foils and the minima correspond to the midpoints of the foils. Near the edge of the reactor the flux rises abruptly due to the inadequacy of diffusion theory near a boundary. Near the center of the reactor the flux rise is associated with the lowered fuel concentration due to the structural modifications occasioned by the control and safety rod systems. It is seen that the amplitude of the flux oscillation is small in the plane of the fuel foils. We believe that in the transverse direction the amplitude is smaller, and that when this oscillation is translated into a change in equivalent fuel loading, the change is second order and negligible.

Figure 10 displays the disadvantage factor curves for the D_2O system and graphite/oralloy systems with $(C/U)_{nominal}$ of 600:1, 1200:1, 2340:1. The following table lists the $(C/U)_{nominal}$, fuel foil thickness, D.F., $(C/U)_{eff.}$ This $(C/U)_{effective}$ is the C/U that would be required to make a homogeneously loaded system (oralloy, graphite of $\bar{\rho} = 1.63$) of the same size critical.

$(C/U)_{Nominal}$	Fuel Foil Thickness Mils	D.F.	$(C/U)_{Effective}$
$(C/U)_{p\text{-assembly}}$	2.08	.768	$1.302\ (C/U)_{p\text{-assembly}}$
600	2.08	.889	675
1200	2.08	.870	1379
2340	1.06	.905	2586

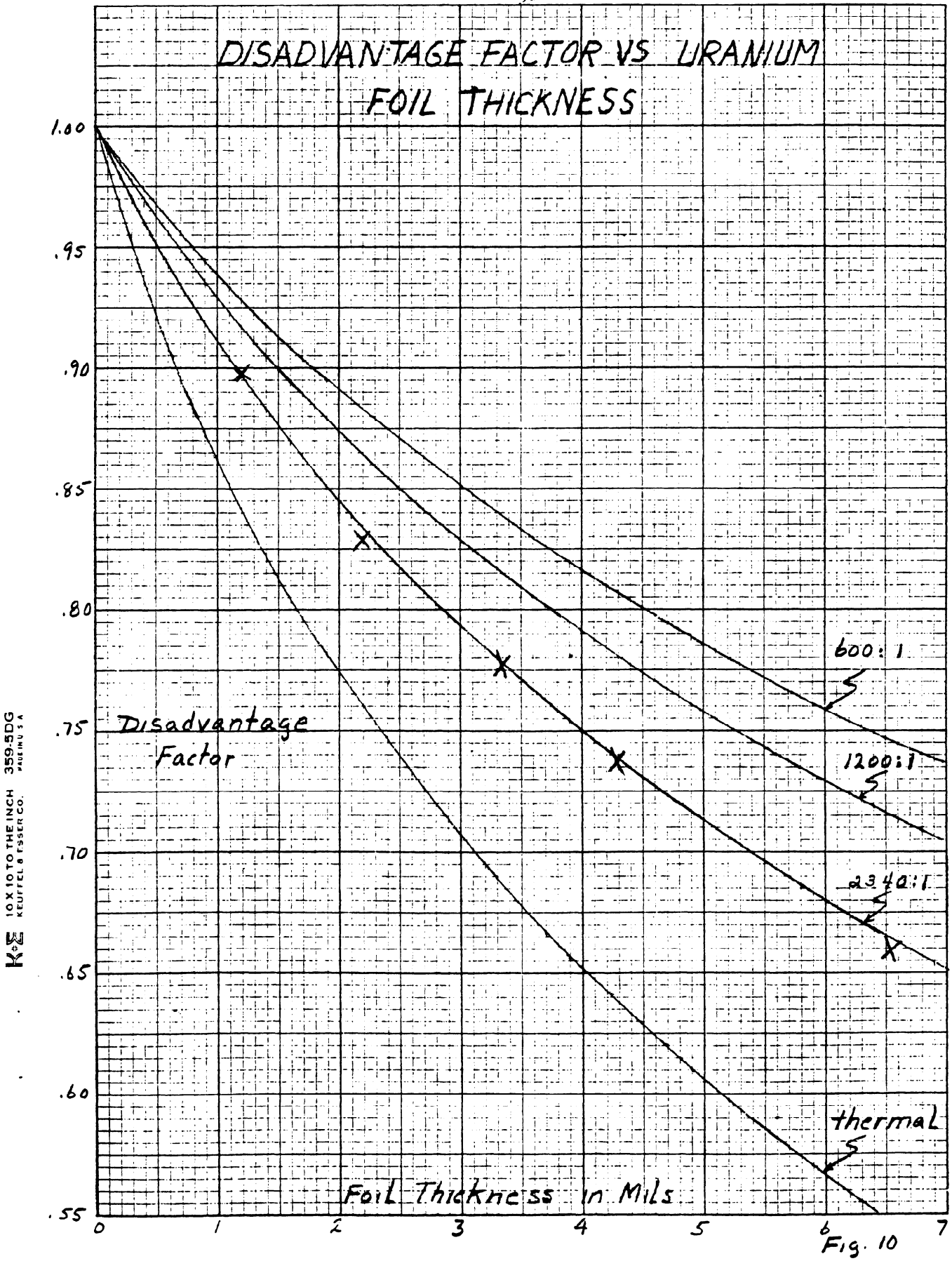
DISADVANTAGE FACTOR VS URANIUM FOIL THICKNESS
1.00
.95
.90
.85
.80
.75
.70
.65
.60
.55
Disadvantage Factor
600:1
1200:1
2340:1
thermal
0
1
2
3
4
5
6
7
Foil Thickness in Mils
KE 10 X 10 TO THE INCH 359-5DG KEUFFEL & ESSER CO. MADE IN U.S.A.

Fig. 10

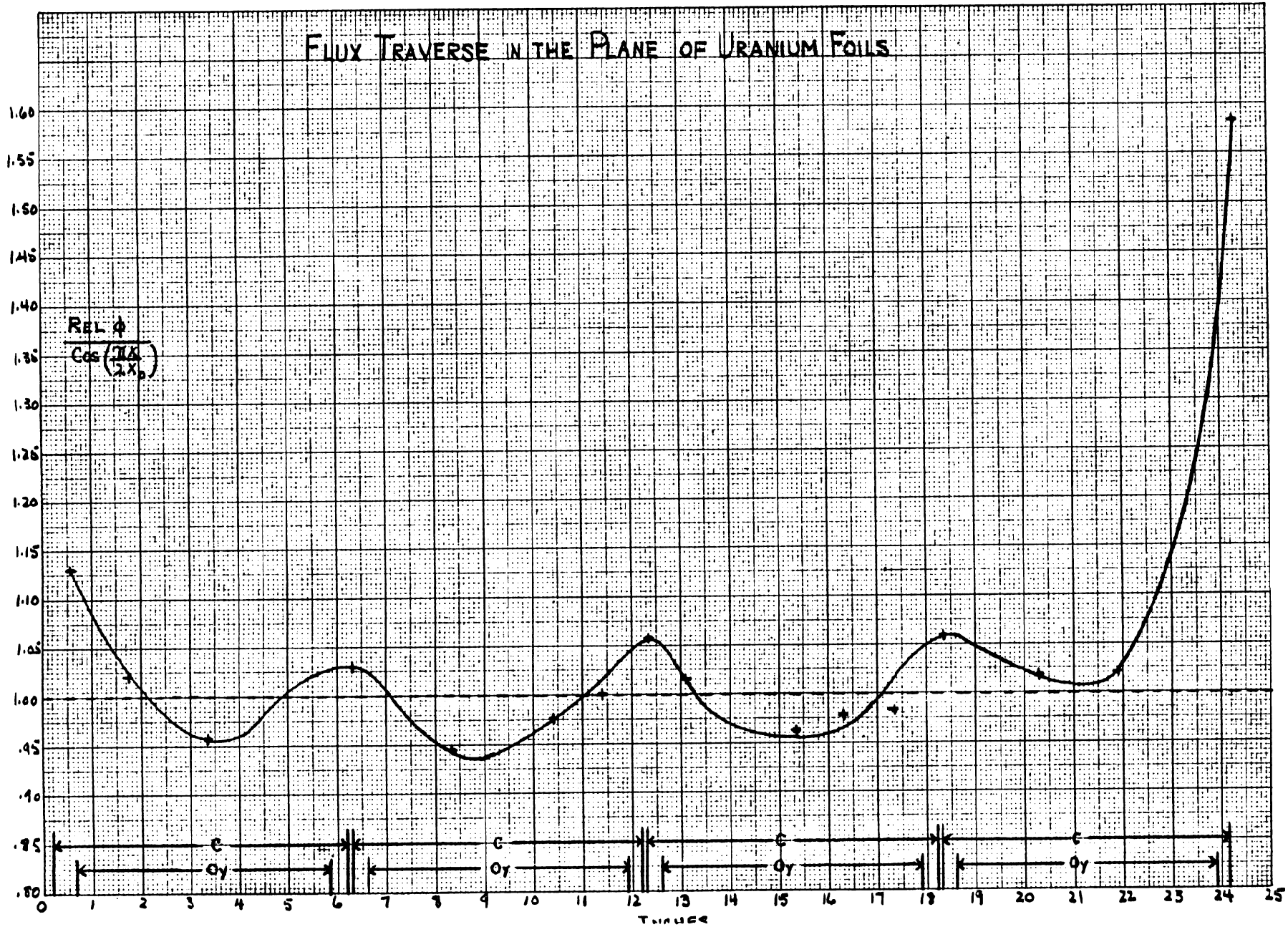

UCRL-4983-T